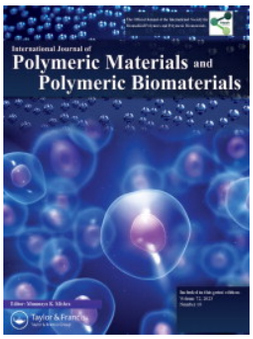

International Journal of Polymeric Materials and Polymeric Biomaterials

ISSN: (Print) (Online) Journal homepage: https://www.tandfonline.com/loi/gpom20

Applying quality by design approach for the determination of potent paclitaxel loaded poly(lactic acid) based implants for localized tumor drug delivery

Ece Özcan Bülbül, Neslihan Üstündağ Okur, Duygu Mısırlı, Erdal Cevher, Vasilios Tsanaktsis, Özlem Bingöl Özakpınar & Panoraia I. Siafaka

To cite this article: Ece Özcan Bülbül, Neslihan Üstündağ Okur, Duygu Mısırlı, Erdal Cevher, Vasilios Tsanaktsis, Özlem Bingöl Özakpınar & Panoraia I. Siafaka (2022): Applying quality by design approach for the determination of potent paclitaxel loaded poly(lactic acid) based implants for localized tumor drug delivery, International Journal of Polymeric Materials and Polymeric Biomaterials, DOI: 10.1080/00914037.2022.2067538

To link to this article: https://doi.org/10.1080/00914037.2022.2067538

Published online: 26 Apr 2022.

INTERNATIONAL JOURNAL OF POLYMERIC MATERIALS AND POLYMERIC BIOMATERIALS
https://doi.org/10.1080/00914037.2022.2067538

Applying quality by design approach for the determination of potent paclitaxel loaded poly(lactic acid) based implants for localized tumor drug delivery

Ece Özcan Bülbül[a], Neslihan Üstündağ Okur[b], Duygu Mısırlı[c], Erdal Cevher[d], Vasilios Tsanaktsis[e], Özlem Bingöl Özakpınar[f], and Panoraia I. Siafaka[g,h]

[a]Department of Pharmaceutical Technology, Faculty of Pharmacy, Istinye University, Istanbul, Turkey; [b]Department of Pharmaceutical Technology, Faculty of Pharmacy, University of Health Sciences, Istanbul, Turkey; [c]Department of Biochemistry, Faculty of Pharmacy, University of Health Sciences, Istanbul, Turkey; [d]Department of Pharmaceutical Technology, Faculty of Pharmacy, Istanbul University, Istanbul, Turkey; [e]Faculty of Sciences, School of Chemistry, Aristotle University of Thessaloniki, Thessaloniki, Greece; [f]Department of Biochemistry, Faculty of Pharmacy, Marmara University, Istanbul, Turkey; [g]School of Health Studies, KES College, Nicosia, Cyprus; [h]Faculty of Pharmacy, European University Cyprus, Nicosia, Cyprus

ABSTRACT

In the present study, poly(lactic acid) (PLA) and poly(ethylene succinate) (PESu) or poly(ethylene glycol) (PEG) under the framework of quality by design, were blended to produce effective sustained-release matrices for Paclitaxel delivery. A complete physicochemical characterization including weight variation, thickness, water uptake, moisture absorption, moisture loss, and hydrolytic degradation under physiological conditions, was performed. Quality by design approach was applied to study the critical parameters. *In vitro* cancer toxicity was studied in human cancer cell lines including lung and breast adenocarcinoma. The developed Paclitaxel-loaded films can act as a promising alternative topical matrix as an implant for breast and lung cancer treatment.

GRAPHICAL ABSTRACT

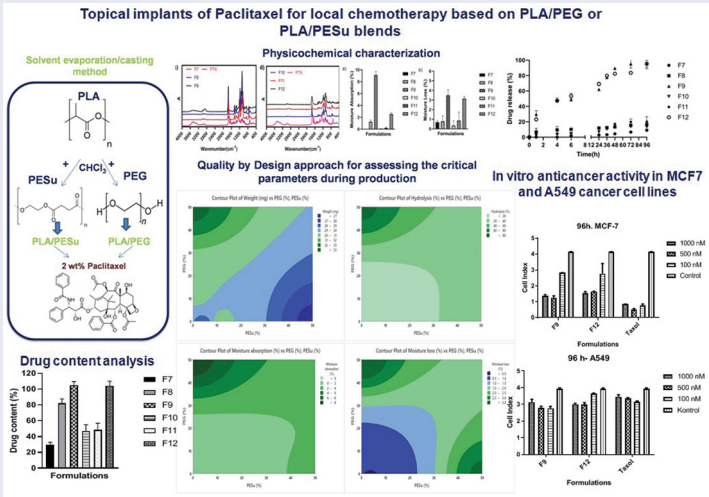

ARTICLE HISTORY
Received 10 February 2022
Accepted 13 April 2022

KEYWORDS
Breast cancer; cancer treatment; film; lung cancer; paclitaxel; quality by design

1. Introduction

According to the World Health Organization (WHO), an estimated 9.6 million deaths occurred in 2018, due to cancer. It has been reported that lung cancer is the most fatal cancer type[1]. There are two basic types of lung cancer existing, non-small-cell lung cancer (NSCLC) and small-cell lung carcinoma (SCLC)[2]. Taxol containing the active ingredient paclitaxel (PTX) is widely used as the standard first-line chemotherapeutic drug in the treatment of NSCLC[3]. Further, according to the WHO, breast cancer is the second most common cancer all over the world after lung cancer[1]. Breast cancer is the most common malignancy in women worldwide, ~10% of it is inherited and ~70–80% of non-metastatic patients have a chance of cure. It is a heterogeneous disease at the molecular level, advanced breast cancer with organ metastases cannot be cured with currently available treatments[4]. MCF-7, a commonly used breast cancer cell line, has been promoted by many research groups for over 40 years. The literature provides a broad description of the MCF-7 cell line, including spheroid formation,

CONTACT Neslihan Üstündağ Okur neslihanustundag@yahoo.com Department of Pharmaceutical Technology, Faculty of Pharmacy, University of Health Sciences, Istanbul, Turkey; Panoraia I. Siafaka siafpan@gmail.com School of Health Studies, KES College, Nicosia, Cyprus.

Table 1. The Quality Target Product Profile (QTPP) of topical drug-loaded films.

QTPP element	Target	Reason
Dosage form	Topical film	Ensuring compliance of the patient
Route of administration	Topical	Appropriate application route for the films
Dissolution profile	Must be appropriate	Ensuring compliance of the patients
Stability	Must have consistent stability profile	Ensuring adequate protection until usage of patients
Container system	Airtight aluminum foil	Maintain films integrity

molecular profile, migration, proliferation, invasion, interaction with mesenchymal stem cells, and involvement in angiogenesis and lymphangiogenesis of the MCF7 cell line in breast cancer[5–7]. Management of breast cancer includes locoregional (radiation and surgery) treatment and systemic treatment approaches. Chemotherapy is one of the systemic treatments[4]. PTX is one of the mitotic inhibitors that stop the division of cells used in the treatment of breast cancer[8].

Polymeric films have been prepared as implantable systems for local chemotherapy[9,10]. Local chemotherapy involves the delivery of the anticancer drugs directly to the tumor site, decreasing the adverse effects of the drugs on the surrounded healthy tissues and reducing the extremity of side effects[11]. In this study, poly(lactic acid) (PLA) was blended with poly(ethylene glycol) (PEG) or poly(ethylene succinate) (PESu) to produce efficient mixtures that can be used in the treatment of lung and breast cancer and to study their release rate and other properties. Additionally, in the present study Quality by Design (QbD) was utilized to ensure that the films can be used as potential drug carriers. QbD is a systematic approach to improvement that starts with pre-described goals and emphasizes product and process understanding with quality risk management. In the past years, this approach is used in drug formulations particularly scaling-up procedures as it decreases time spent and charges[12].

In our work, a comparison between different blends of PLA with PEG or PESu as carriers to modify the release profile of the hydrophobic drug, PTX is done. Under the framework of QbD formulated films were prepared using the solvent casting/evaporation technique. The films were comprehensively characterized by various physicochemical methods. The effect of PEG and PESu addition on *in vitro* PTX release and *in vitro* cancer toxicity were tested.

2. Materials and methods

2.1. Materials

PESu, PLA, PTX, and Chloroform were purchased from Sigma–Aldrich, Germany. PEG 400 was supplied by Merck, Germany. High-pressure liquid chromatography (HPLC) grade Acetonitrile (Sigma, Germany) was used for HPLC studies. All other reagents and solvents used were of analytical grade. The dialysis membranes were purchased from Spectrum and presented the following characteristics: Spectra/por 4, $d = 16$ mm, and M_w = 12–14 kDa. QbD was performed using Minitab 19.2020.1.0 software.

Table 2. CMAs and CQAs for topical drug-loaded films.

CMA	CQA
PLA ratio (95, 90, 50%)	Weight
PEG or PESu ratio (5, 10, 50%)	Thickness
	Water uptake
	Hydrolysis
	Moisture absorption
	Moisture loss
	Mechanical properties
	Drug loading
	Drug release (dissolution)

2.2. Application of quality by design

In general, the dosage form, dosage strength, route of administration, pharmacokinetics, and packing system are Quality Target Product Profile (QTPP) elements for films[12,13]. Table 1 presents the QTPP of topical PTX-loaded films and targets. Critical Quality Attributes (CQAs) are represented as a feature that should be within a limit to maintain the desired final product quality[14]. Next, Critical Material Properties (CMA) and Critical Process Parameters (CPP) need to be defined. CMAs are polymer type, polymer ratio, plasticizer type, and plasticizer ratio for films[15,16]. CPPs include drying temperature and drying time that influences the CQAs[15]. QbD was performed with regression analyses using Minitab 19.2020.1.0 software. The summary of CMAs and CQAs of topical PTX-loaded films is given in Table 2.

2.3. Preparation of topical films via solvent evaporation method

PLA/PESu or PLA/PEG films were prepared using the solvent evaporation method as in our previous method[17], employing chloroform as the solvent. The polymers were dissolved using 8 mL chloroform, cast on the glass Petri dishes, and left until full evaporation. To prepare the PTX-loaded films, the drug was theoretically loaded into the films at 2% w/w. Afterward, the film was kept at room temperature to remove the solvent until the constant mass was achieved. The formulation components of films are shown in Table 3.

2.4. Physicochemical characterization of the prepared PLA/PEG and PLA/PESu films

2.4.1. Differential Scanning calorimetry (DSC)

The thermal properties of the prepared polymeric films were studied utilizing a DSC (Perkin Elmer, Pyris Diamond, USA) in a temperature range of 20–240 °C using a heating rate of 10 °C·min^{-1}. The samples (8 mg) were placed in the

Table 3. The exact used amounts of components for the preparation of the topical films.

Formulations	PLA (g)	PEG (g)	PESu (g)	PTX (g)	Total mass (g)	Film
F1	0.95	0.05	0	0	1	PLA/PEG 95/5
F2	0.90	0.10	0	0	1	PLA/PEG 90/10
F3	0.50	0.50	0	0	1	PLA/PEG 50/50
F4	0.95	0	0.05	0	1	PLA/PESu 95/5
F5	0.90	0	0.10	0	1	PLA/PESu 90/10
F6	0.50	0	0.50	0	1	PLA/PESu 50/50
Drug loaded films						
F7	0.931	0.049	0	0.02	1	PLA/PEG 95/5 + 2%PTX
F8	0.882	0.098	0	0.02	1	PLA/PEG 90/10 + 2%PTX
F9	0.490	0.490	0	0.02	1	PLA/PEG 50/50 + 2%PTX
F10	0.931	0	0.049	0.02	1	PLA/PESu 95/5 + 2% PTX
F11	0.882	0	0.098	0.02	1	PLA/PESu 90/10 + 2%PTX
F12	0.490	0	0.490	0.02	1	PLA/PESu 50/50 + 2%PTX

aluminum pans, held at the temperature for 5 min, and then were cooled down at 300 °C·min^{-1} rates. The calibration of the instrument was done with Indium and Zinc standards.

2.4.2. ATR-Fourier-Transformed infrared (FTIR) spectroscopy

The infrared spectra of the polymers, drug, and the prepared films were obtained with ATR-FTIR (attenuated total reflection Fourier transform infrared) spectroscopy (FTIR–spectrometer FTIR–2000 (Perkin Elmer, USA). The developed thin films were placed on the ATR crystal while the possible maximum pressure was applied using a pressure clamp to allow an intimate contact of the films with the ATR crystal. The spectra were recorded from 4,000 to 400 cm^{-1} and they are presented as baseline corrected in absorbance mode.

2.4.3. Weight and thickness

The fabricated films were circle-shaped with a diameter of 1.6 cm ($n = 5$) and the determination of their weight was performed using a microbalance[12].

2.4.4. Water uptake

The water uptake was carried out by immersing the films (1.6 cm in diameter) in 10 g of distilled water at 25 °C. After 60 min, the hydrated films were removed from the water, the surface water extracted using filter paper and the films weighed.

2.4.5. In vitro hydrolysis studies of films

The hydrolysis degree of the developed films was associated with mass loss. For this reason, the circular-shaped films ($d = 1.6$ cm) were placed in Petri dishes with phosphate buffer solution (pH 7.4). The incubation period of the films was 5 days at 37 ± 1 °C. Every 24 h, the films were removed from the Petri dishes, washed with distilled water, dried (at room temperature until reaching a constant weight), and weighted[18].

2.4.6. Percentage of moisture absorption

For the evaluation of the physical stability of the films ($d = 1.6$ cm) in high humidity conditions, the films were accurately weighed and placed in a desiccator containing a saturated solution of potassium chloride (34 g potassium chloride in 100 ml distilled water) for 3 days.

2.4.7. Percentage of moisture loss

The percentage of moisture loss from the freshly prepared film was performed as follows: The circular-shaped films were accurately weighed and placed in a desiccator containing 100 g silica gel.

2.4.8. Mechanical properties

The mechanical properties of the selected films according to previous studies ($n = 3$) were carried out with a texture analyzer (TA.XTPlus, Stable Micro Systems, UK) with a load cell of 2 kg. The film (1 × 5 cm) was placed between clamps at a distance of 3 cm. Clamps were moved from each other until the breakage of the films with a crosshead speed of 0.5 mm·s^{-1}. The elongation at break (%), Young's modulus, and tensile strength were calculated[12,19,20].

2.4.9. High-performance liquid chromatography (HPLC) analysis

For the HPLC analysis, a previously reported method was chosen[21–25]. The HPLC system (Prominence-I LC-2030C 3 D Plus Liquid Chromatograph) is comprised of a gradient pump and a UV detector. The chromatographic separation was achieved with a C18 column (Intersil ODS-3 5 µm, 150 × 4.6 mm, GL Sciences, Japan) with the temperature set at 25 °C.

2.4.10. Drug content and in vitro drug release

The drug content estimation was performed using the above described HPLC methodology. The circular-shaped films ($d = 1.6$ cm) were grounded in a glass pestle mortar, dissolved in methanol ($V = 10$ mL), and mixed with a magnetic stirrer for 24 h. The obtained solution was filtered through PTFE membrane filters (0.45 µm). The experiments were performed at 25 ± 2 °C in triplicate and their average index is presented.

In vitro release study was carried out by placing the circular-shaped films in 10 ml of methanol/phosphate buffer (pH 7.4) mixture at a ratio of 50/50 (v/v), acting as dissolution medium, at 37 ± 0.5 °C and 50 rpm[17]. At specific time intervals, 0.5 ml of the media was removed, and the same volume of fresh medium was added. The experiments were carried out three times and the average release percentage (%) is presented.

2.4.11. Kinetic analysis data

Further, *in vitro* release study was correlated and analyzed with various kinetic models[26]. By analyzing the *in vitro* dissolution behavior with the available mathematic models can be useful for predicting the possible *in vivo* performance of the films. Herein, a computer-based kinetic software[27] was applied to decide which kinetic model is the most suitable for describing the dissolution behavior. Various mathematical models as described follows were correlated with the *in vitro* release data; the fitting of dissolution behavior and the mathematical models indicated by the supremacy of the coefficient of determination large value (r^2)[17,28].

2.4.12. Morphology observation of the films using microscopy

The morphological examination of the PTX-loaded films was carried out with a microscope ZOE Fluorescent Cell Imager (BIO-RAD). In addition, Scanning Electron Microscopy (Hitachi SU 7000) was also employed for the characterization of morphological features of the prepared films.

2.4.13. Cancer cell culture—cell viability assay

2.4.13.1. Cell culture. The human lung and breast adenocarcinoma cell lines A549 and MCF 7 were obtained from the ATCC and maintained according to the recommendations of the ATCC at 37 °C and 5% CO_2 in complete DMEM, supplemented with 100 U·mL^{-1} penicillin G, 100 µg·mL^{-1} streptomycin and 10% FBS. After reaching confluence, the A549 and MCF 7 cells were detached using 0.25% trypsin-EDTA, and 1×10^4 cells were seeded into the 48 well plates.

2.4.13.2. Cell viability assay. xCELLigence® RTCA assay was performed by initially seeding 1×10^5 cells/mL of A549 and MCF 7 cells on gold microelectrode precoated 48 well electronic plates (E-Plate® 48, ACEA Biosciences Inc., San Diego, CA, USA) and incubating at 37 °C in 5% CO_2 (v/v) for 24 h. Nanomaterial (Coded F9 and F12) containing PTX and pure PTX in 1,000, 500, and 100 nanomolar concentrations were added to the wells. Untreated cells (containing medium only) were included as a negative control. The cell cultures were then incubated for a further 96 h, with impedance measurements were taken every 15 min during the total incubation period of 96 h. Cell viability was calculated with the graph obtained and presented graphically. All assays were done in triplicate and experiments were repeated three different times.

3. Results and discussion

3.1. Miscibility studies of PLA/PEG and PLA/PESu blends based on FTIR and DSC analyses

Polymeric blends as pharmaceutical formulations have been recently introduced due to their great physicochemical behavior. For example, the blends can be applied to alter the drug release behavior. The polymer blends can be produced with a variety of methods, such as solvent evaporation, electrospinning, melt mixing, etc.[17,18,29]. A very important factor attributing to drug release behavior is polymer blends and their associated miscibility. Immiscibility can affect the release behavior since immiscible blends could vigorously release the drug due to the developed empty channels between the polymer phases. On the other hand, miscible blends could release the molecules in a controllable manner[30,31]. Accordingly, the prepared PLA/PEG and PLA/PESu blends were studied using DSC and FTIR methods. It should be mentioned that the miscibility, partial or full, as well as immiscibility of the blends, are based on the depiction of one single-phase; thus, miscibility can be obtained when one melting point (T_m) or glass transition temperature (T_g) recorded in DSC thermograms. The temperatures range temperatures between those corresponding to the initial polymers, are similar or at even higher temperatures[17,18,29,32]. Figure 1a shows the DSC thermograms of F1, F2, and F3 formulations which are based on PLA/PEG. It is well-known that PLA is a semi-crystalline polymer providing the T_g at 53 °C as well as a T_m at 153 °C while PEG presents a T_m around 66 °C[33]. In the past, PEG has been proposed as a plasticizer in various polymer blends; plasticizers are used as additives to make them softer and more flexible[34]. As can be seen, both F1 and F2 comprised 5 and 10% PEG, showing T_m around 153 °C which is attributed to PLA, and the cold exothermic peak of cold crystallization (T_{cold}) around 122 °C. In the case of F3 composed of 50% PEG, a T_m around 125 °C; the suppression of the T_m could be associated with partial miscibility since PEG displayed a plasticizing effect.

PESu is also a semi-crystalline polyester with a lower T_g value at −55 °C, and one melting endotherm (101 °C) with one shoulder (91 °C)[17,35]. From Figure 1b, it can be seen that F4 and F5 could present possible miscibility considering that the T_m of PESu T_m has not been depicted but the T_m point of PLA is ascribed at 153 °C with a shoulder at 147 °C. Nonetheless, it is possible that the PESu concetration is quite low and cannot be detected[18,29]. In the case of F6, the T_m of PESu can be seen at 99 °C with a shoulder at 91 °C while the T_m of PLA has been shifted to higher temperatures. Consequently, the specific blend is immiscible, probably due to the crystallization of PESu in the amorphous PLA matrix. Similar results were observed in our previous study[17].

FTIR spectroscopy belongs to the handful of methodologies for the examination of pharmaceutical formulations. FTIR spectrum can exhibit possible interactions between the components and possible stability. Besides, the possible interactions can generate newer or undesirable products.

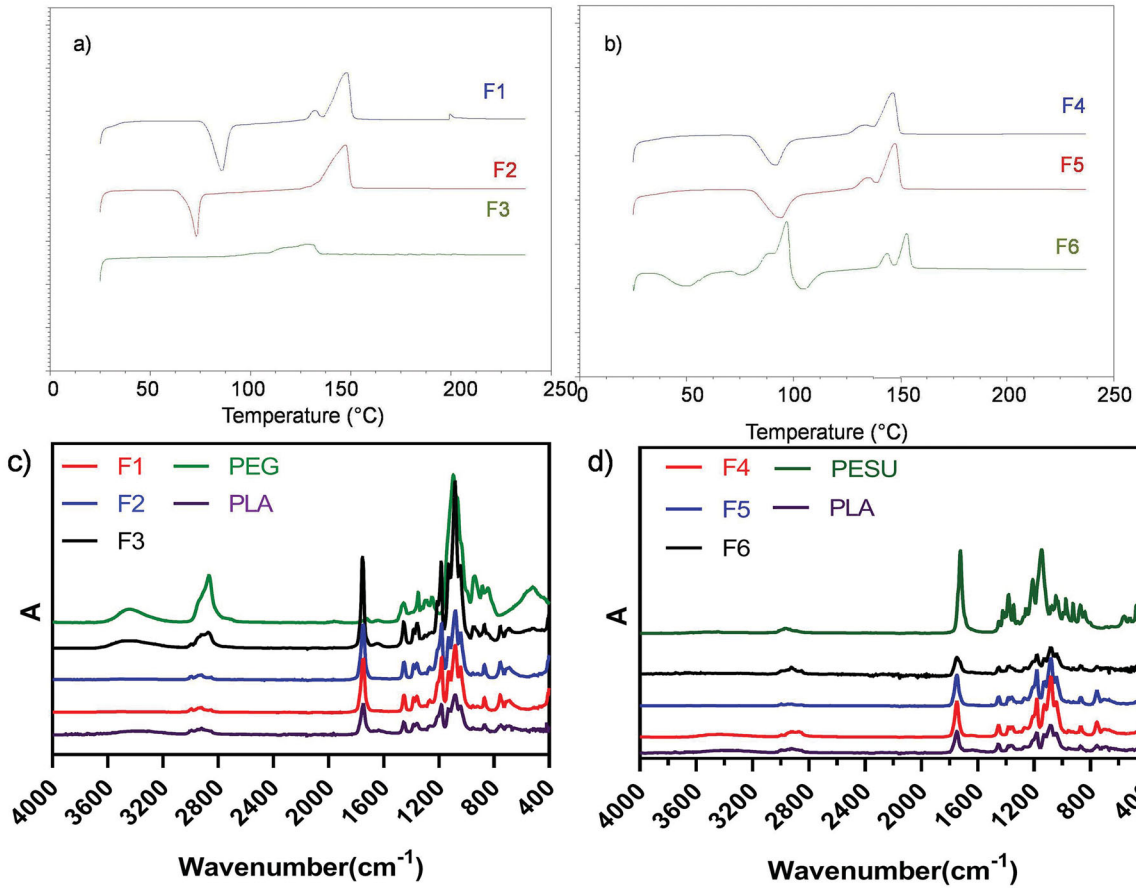

Figure 1. DSC thermograms of (a) F1, F2, and F3, (b) F4, F5, F6, and FTIR spectra of (c) PLA, PEG, and F1, F2, F3 formulations, and (d) PLA, PEG, and F4, F5, F6 formulations.

Moreover, the interactions can affect the miscibility of the blends. Figure 1c demonstrates the FTIR spectrum of PLA, PEG as well as their associated blends. PLA is an aliphatic polyester; its spectrum exhibits the following frequencies: C=O (1,743 cm^{-1}), $-CH_3$ asymmetric (2,996 cm^{-1}), $-CH_3$ symmetric (2,945 cm^{-1}), and C–O (1,081 cm^{-1}). Also, the bending frequencies for $-CH_3$ asymmetric and $-CH_3$ symmetric can be found at 1,451 and 1,362 cm^{-1}[18,36]. PEG depicts a broad peak at 3,446 cm^{-1}, which is associated with the terminal hydroxyl group[37]. F1 and F2 have almost the same absorption peaks as pure PLA. However, the addition of 50% PEG altered the spectrum of F3 which presents both PLA and PEG characteristics peaks. This could be associated with the increased concentration of hydrophilic PEG. Although the characteristic bands of PEG displayed in lower wavenumbers, i.e., the broadband of hydroxyl groups was depicted in 3,442 cm^{-1} instead of 3,446 cm^{-1}, it cannot safely conclude possible interaction or miscibility. Nonetheless, the formation of new bonds or strong chemical interactions was not observed demonstrating possible stability and compatibility between the components[29,36]. In Figure 1d, the obtained spectra of the developed PLA/PESu films are revealed. Similar to our previous study, PESu spectra present two peaks of 1,742 and 1,736 cm^{-1} associated with the absorbance of PESu in amorphous and crystalline domains, respectively[38]. The spectra of F4, F5, and F6 follow the spectrum of PLA. Nonetheless, some of the bands shifted in lower wavenumbers closely to that of PESu which however cannot conclude safely any interactions[18,29].

3.2. Characterization of the drug-loaded PLA/PEG and PLA/PESu films with DSC and FTIR analyses

The dissolution behavior of a drug is related to its physical state. Amorphous drugs can be easily dissolved while crystalline drugs present very low solubility[37]. Amorphous drugs can be developed via various techniques; rapid solvent evaporation belongs to them. Figures 2a and 2b exhibited the DSC thermograms of the PTX-loaded formulations. It is well-known that PTX presents a T_m at around 224 °C. Herein, the T_m of PTX was absent suggesting amorphization of the drug[17,39]. In some cases, the amorphization of the drug which leads to improved dissolution is associated with strong interactions between the components. However, in this work, the amorphization could have taken place due to the fine dispersion of the drug or rapid solvent evaporation. Also, comparing the melting points of the PTX loaded and neat blends, any shifting was not observed, indicating that the drug did not play any role as plasticizing agent. Similar results have been observed when the lipophilic and crystalline drug, voriconazole was incorporated in PLA/PESu blends[17].

PTX is an antitumor lipophilic drug with high crystallinity, as has been previously reported[40]. Theoretically, the drug

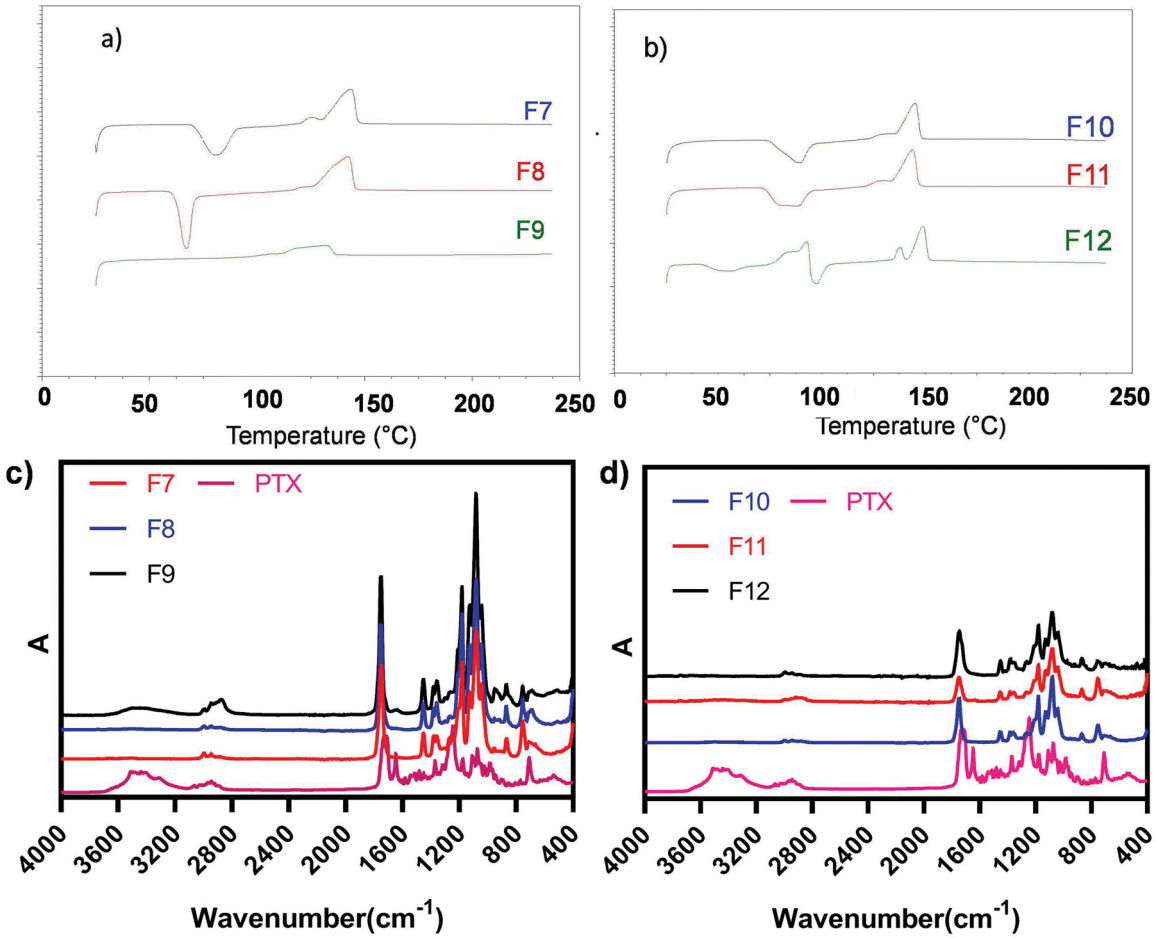

Figure 2. DSC thermograms of PTX loaded formulations (a) F7, F8, F9, and (b) F10, F11, F12, and FTIR spectra of (c) F7, F8, F9 formulations, and PTX drug and (d) F10, F11, F12 formulations, and PTX drug.

loading of PTX into the formulations was 2% w/w. Figures 2c and 2d demonstrate the FTIR spectra of PTX as well as formulations. PTX spectrum comprised of the N-H stretching vibrations at 3,500–3,300 cm^{-1}, CH_2 asymmetric, and symmetric stretching vibrations at 2,976–2,885 cm^{-1}. The C = O stretching vibration from the ester groups can be seen at 1,733 cm^{-1} while the amide bound is at 1,648 cm^{-1}. Similar results have been shown in previous studies[41]. It can be said that the spectra of the prepared PTX loaded formulations followed the order of the neat blends. Any evidence of new bands or shifting could not be observed. This can suggest compatibility between the polymeric components and the PTX drug.

3.3. Physicochemical parameters of the prepared films (weight, thickness, water uptake, in vitro hydrolysis rate, moisture absorption, and moisture loss)

3.3.1. Weight and thickness

Weight and thickness are important parameters when pharmaceutical products are prepared. Besides, thin films have been associated with patient compliance, therapeutic efficiency, reduced dose frequency, etc.[42]. Table 4 shows the mean weight and thickness of the prepared formulations. The average weight of films was in the range of 26.62 ± 2.92–33.36 ± 1.49 mg whereas the average thickness was between 0.09 ± 0.03 and 0.16 ± 0.03 mm. Similar to our study, the thickness of the mats prepared by Okur et al. in the ratio of 90/10 and 50/50 with a mixture of PLA and PESu was found between 0.09 and 0.1 mm[17]. The SD values of both weight and thickness of films were found very low revealing that the weight and thickness of the films are uniforms[12]. It has been reported that a large variation in weight demonstrates that the applied fabrication method could be inefficient while there is a high chance that drug content would also be non-uniform[43]. Consequently, the solvent evaporation method can prepare uniform formulations and it can be used as a formulation methodology.

Table 4. Weight and thickness of the films (mean ± *SD*, *n* = 5).

Formulation	Weight (mg)	Thickness (mm)
F7	29.70 ± 1.34	0.11 ± 0.01
F8	30.82 ± 1.45	0.11 ± 0.01
F9	33.36 ± 1.49	0.09 ± 0.03
F10	27.86 ± 1.35	0.09 ± 0.01
F11	30.78 ± 4.32	0.13 ± 0.02
F12	26.62 ± 2.92	0.16 ± 0.03

3.3.2. Water uptake and in vitro hydrolysis studies

Among other parameters, the water uptake is also significant during the development of topical films. It can be said that the films can absorb water (Figure 3a). It is depicted that by increasing PEG content the water uptake, decreased for

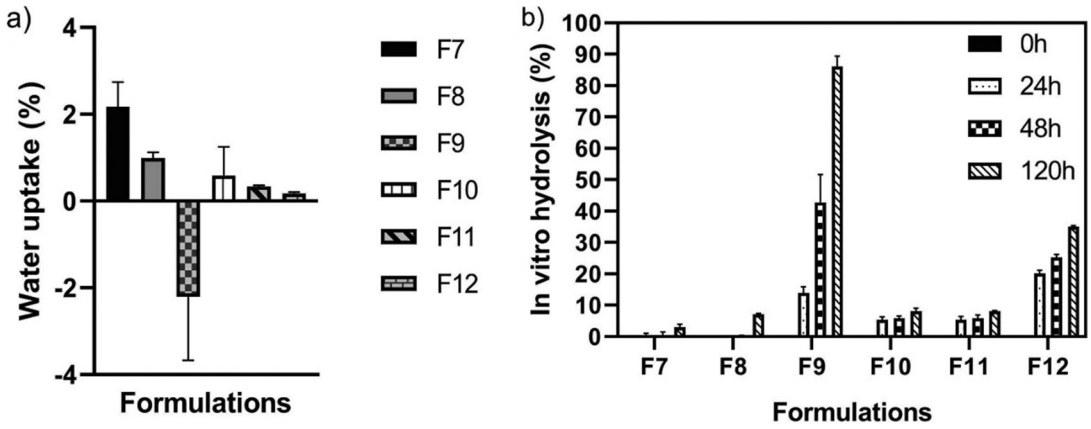

Figure 3. (a) Water uptake of the films ($n = 3$) and (b) *In vitro* hydrolysis degree (%) of films ($n = 3$).

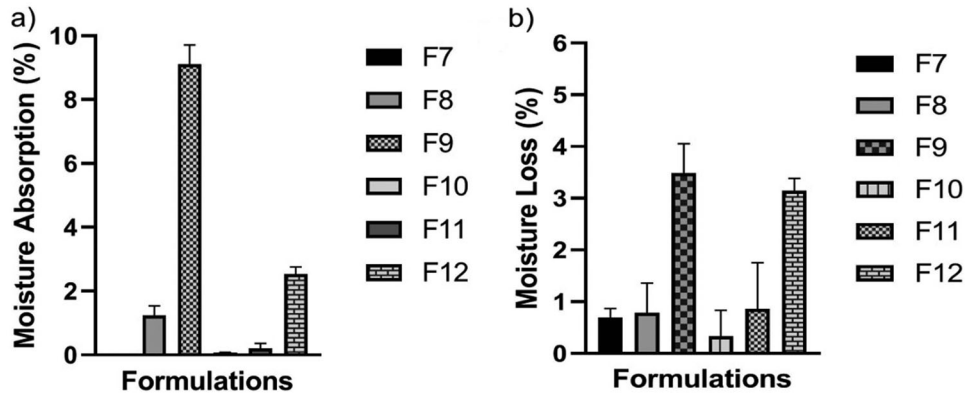

Figure 4. (a) Moisture absorption percentage of films ($n = 5$) and (b) Moisture loss percentage of films ($n = 5$).

PLA/PEG formulations. The water uptake of 95/5 (F7), 90/10 (F8), and 50/50 (F9) PLA/PEG was found at 2.18, 0.99, and −2.20%, respectively. In the F9 formulation, the ratio of PEG is higher than the others (PLA/PEG 50/50). Since PEG is dissolved in water, the mass reduction will likely occur. Therefore, a negative value was found. In case of 95/5 (F10), 90/10 (F11) and 50/50 (F12) PLA/PESu water uptake was found similar (0.59, 0.34, and 0.18%, respectively). There was almost no water intake in the PLA/PESu formulations because both PLA and PESu are hydrophobic materials[17].

In vitro hydrolysis studies (Figure 3b) are very important in pharmaceutical technology since the hydrolysis rate can predict and be linked with the dissolution behavior. Herein, 95/5 PLA/PEG (F7) could not be fully degraded when in contact with the hydrolysis medium. F7 hydrolyzed at 3.30% in 120 h. Similar behavior was found for 90/10 PLA/PEG (F8) film with a slightly higher hydrolysis degree in 120 h (7.27%). Both 95/5 PLA/PESu (F10) and 90/10 PLA/PESu (F11) degraded only 8% while 50/50 PLA/PESu (F12) depicted a higher degradation rate as it was reported in a study[17]. In this study by Okur et al., hydrolysis increased as the amount of PESu increased in mats prepared with PLA and PESu polymers, as in our study[17]. Finally, similar behavior was indicated for 50/50 blend PLA/PEG (F9), which presents the highest degree of hydrolysis (86.46%) in 120 h. PEG seems to improve hydrolysis as has been reported in the literature. For example, a study demonstrated that the addition of glycerol in films remarkably decreased the solubilization time considering that the hydrophilicity of the film was improved due to the presence of hydroxyl groups of extra glycerol[44]. Subsequently, in the current study, the increased amount of PEG led to a higher hydrophilicity and hydrolysis degree.

3.3.3. Percentage of moisture absorption and moisture loss

There was almost no moisture absorption (Figure 4a) for 95/5 PLA/PEG (F7), 95/5 PLA/PESu (F10), and 90/10 PLA/PESu (F11) formulations. Different behavior was indicated for 50/50 PLA/PEG (F9), which presents the highest moisture absorption (9.11%). Generally, it was seen that the increase in the PEG amount causes an increase in the percentage of moisture absorption of films. Similarly, a study reported that as the number of hydrophilic polymers increases, moisture absorption increases[45].

In 95/5 PLA/PEG (F7), 90/10 PLA/PEG (F8), 95/5 PLA/PESu (F10), and 90/10 PLA/PESu (F11) formulations, moisture loss was below 1% (Figure 4b). 50/50 PLA/PEG (F9) presented the highest moisture loss (3.48%). Generally, it was seen that the increase in the PEG amount causes an increase in the percentage of moisture loss of films.

Table 5. Mechanical properties of the films (mean ± *SD*, $n = 3$).

Formulation	Tensile strength (MPa)	Young's modulus (MPa/%)	Elongation at break (%)
F7	10.875 ± 0.456	1.538 ± 0.070	25.065 ± 1.336
F8	8.816 ± 1.088	1.496 ± 0.058	32.885 ± 0.672
F9	3.112 ± 0.523	0.692 ± 0.094	40.675 ± 2.157
F10	11.397 ± 1.079	1.607 ± 0.226	28.440 ± 3.940
F11	6.066 ± 0.785	1.091 ± 0.118	12.967 ± 1.831
F12	0.659 ± 0.275	0.280 ± 0.108	2.747 ± 0.599

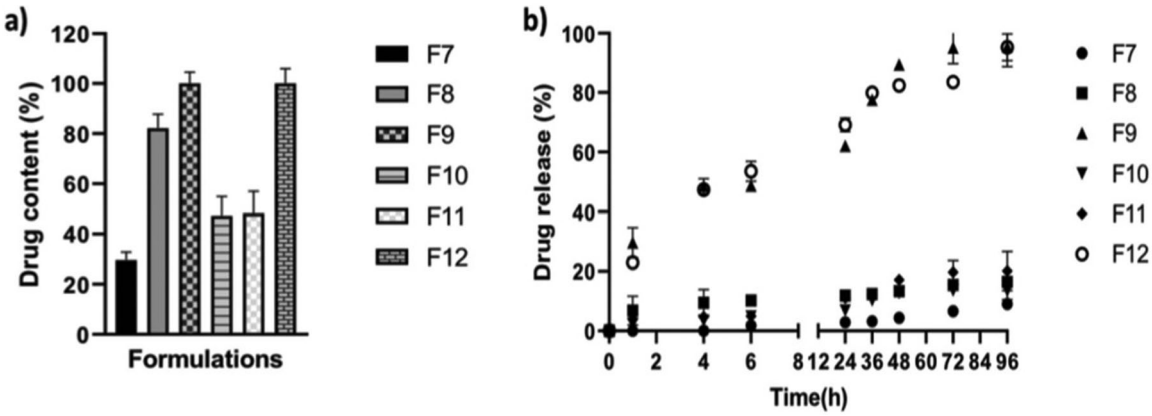

Figure 5. (a) Drug content of the films and (b) *In vitro* release profile of PTX from the films.

3.4. Mechanical properties of the prepared films

The mechanical properties of films are significant for dissolution behavior, handling procedures, stability, and packing[12,46]. Accordingly, the tensile strength, Young's modulus, and elongation at the break of the prepared films were calculated and listed in Table 5. The tensile strength is the maximum stress that a film can withstand being stretched before cracking. It can be declared that films that give higher tensile strength correspond to a more powerful film[19]. In this study the highest tensile strength was higher in the case of F10 (11.397 ± 1.079 MPa), followed by F7 > F8 > F11 > F9 > F12. Similarly, the highest Young's modulus was that of F10 film (1.607 ± 0.226 MPa/%) followed by F7 > F8 > F11 > F9 > F12. The highest elongation at break was that of F9 film (40.675 ± 2.157%) followed by F8 > F10 > F7 > F11 > F12. By adding a plasticizer to a polymeric material, elongation at break is expected to increase, on the other hand, tensile stress and Young's modulus are expected to decrease[47–49]. Pivsa-Art et al. reported that this effect was stronger with increased PEG content[34]. Similarly, also in our study, as PEG was added to the PLA formulations, the tensile strength, and Young's modulus decreased and the amount of elongation increased (F7, F8, and F9). Moreover, the highest elongation was seen in the formulation containing the most PEG (F9), as expected. As PESu was added to the PLA formulations, the tensile strength, and Young's modulus decreased (F10, F11, and F12). These similar situations were also reported in poly(L-lactide) (PLLA)/PESu blends[50] and poly(3-hydroxybutyrate-co-hydroxy valerate) (PHBV)/(PESu) blends[51]. The values of elongation at break decreased with increasing PESu content (F10, F11, and F12). According to the above information, F9 offered good tensile strength, Young's modulus, and high elongation properties that are ideal for films.

3.5. Drug content and in vitro drug release studies

The average content of PTX (%) was found between 29.68 and 100% (Figure 5a). The SD in respect of the PTX content was between 3.14 and 8.87. The results are quite rational considering that the solvent evaporation technique is used for great drug loading efficiency[17]. It has been reported that the release rate should be studied along with the hydrolysis behavior or drug amorphization since if the hydrolysis degree of the polymer films is increased then the drug releases faster while the drug can be diffused more rapidly when it is in a rubber state than the glassy state[18,29,52]. Moreover, the miscible blends prolong the release in contrast to immiscible blends which demonstrate rigorous release due to obtained free channels between the polymeric matrices[18,29]. In further, the use of less hydrophobic polymers such as PESu or hydrophilic polymers such as PEG can increase the hydrolysis rate of hydrophobic polymers, such as PLA. As shown in Figure 5b, the film containing more PESu or PEG demonstrated quicker release when compared to the other films. Moreover, all the films were not dissolved. 90% of the PTX was released from 50/50 PLA/PEG (F9) and 50/50 PLA/PESu (F12) formulation within 96 h. Finally, F9 and F12 presented the highest drug release. After 96 h, PTX was ∼10% dissolved from 90/10 PLA/PESu (F11) formulations. Similarly, in the 84-h release study by Okur et al., 50/50 PLA/PESu mats released almost 100% drug, and 90/10 PLA/PESu mats released ∼10% of the drug[17]. From the above, it can be assumed that adding PESu and PEG leads to improved drug release drugs

Table 6. The obtained kinetic analysis data of PTX release parameters.

	Zero order			First order			Higuchi			Hixxon Crowell			Korsmeyer-Peppas	
	r^2	n	m	r^2	n	m	r^2	n	m	r^2	n	m	r^2	n
F7	0.979	0.831	0.0813	0.976	4.597	−0.0009	0.894	−1.599	0.973	0.977	0.012	0.001	0.896	0.560
F8	0.898	8.864	0.0876	0.908	4.512	−0.001	0.961	6.909	0.981	0.905	0.141	0.001	0.969	0.176
F9	0.843	44.632	0.6601	0.951	4.151	−0.031	0.948	28.955	7.576	0.931	0.758	0.027	0.931	0.229
F10	0.859	3.994	0.1250	0.864	4.564	−0.001	0.948	1.093	1.421	0.863	0.062	0.002	0.923	0.408
F11	0.919	4.986	0.187	0.927	4.554	−0.002	0.970	0.878	2.085	0.924	0.077	0.003	0.943	0.409
F12	0.760	45.150	0.602	0.926	4.100	−0.024	0.901	29.862	7.103	0.902	0.798	0.022	0.917	0.345

probably due to the empty channels obtained due to the immiscibility of the polymers. Finally, both F9 and F12 have the greatest drug loading percentage; in the past, it has been reported that by increasing drug loading, the release rate is significantly improved[29].

3.5.1. Kinetic analysis data

It is well-reported that *in vitro* release kinetics can only predict the possible release behavior that the formulations will have when will contact the biological fluids or tissues. Consequently, by analyzing the *in vitro* release data with kinetic models could show how the films will possibly behave. Generally, the main driving forces of drug transportation from a polymeric matrix, have been suggested phenomena, such as diffusion, polymeric matrix swelling, and material degradation[53]. The numerous mathematical models could simplify the complex release process and predict the release mechanism[54]. Normally the mathematical models mainly focus on one or two dominant driving phenomena. As expected, although the kinetic models can describe simple polymeric drug delivery systems when more complex systems are utilized, modeling could be insufficient. In the case of biodegradable systems, such as the prepared PLA/PEG and PLA/PESu films, the water is an important factor during the hydrolysis process; consequently, water intrusion into the device is significant for release kinetics study. Especially when semicrystalline polymers are employed degradation occurs in two stages. Firstly, the water is infused into the amorphous regions with random hydrolytic scission of labile bonds, such as ester bonds, and secondly, the amorphous regions are degraded. The most identified transport mechanisms for degradable systems are diffusion, degradation, and erosion while the zero-order mathematical model is fitted[17]. Herein, the data obtained from *in vitro* release studies of F7, F8, F9, F10, F11, and F12 films were evaluated according to the zero-order, first-order, Higuchi, and Hixson Crowell, and Korsmeyer-Peppas kinetic models. For F7 both zero-order, first-order and Hixson Crowell models could be applied because the r^2 values were very close to each other as 0.9792, 0.9766, and 0.9775, respectively (Table 6). In the case of F8, F10, and F11 films, the release data were fitted to the Higuchi models while for F9 and F12 the r^2 value is higher for the first-order model compared to Hixson Crowell and Higuchi models. Although F12 fitted better to the first-order model, it can be said that none of the models perfectly describe the release mechanism for the specific film. In the past, PLA implants for levonorgestrel were also fitted to first-order release[55]. Similarly, PLGA intraocular polymeric implant systems loaded with clindamycin phosphate complied with first-order kinetics[56]. It can be said that hydrolysis was negligible for F7, F8, F10, and F11, thus their release mechanism is not driven due to erosion or swelling. More specifically, since the Higuchi model is fitted then the drug release mechanism is based on the diffusion of the drug[57].

In vitro release kinetics of PTX-loaded films were also evaluated according to the Korsmeyer-Peppas model[58,59]. The n value of the F7 film was determined as 0.5605 (Table 4) implying that the drug can both diffuse and transport non-Fickian. The drug release for the other films was primarily based on Fickian diffusion transport as suggested by Korsemeyer–Peppas kinetics with n-value < 0.5[60]. An n-value <0.5 can be found for a non-swellable matrix with release driven by diffusion.

3.6. Evaluation of quality by design approach

Favorably to ICH Q9, CMAs, different polymer types, and different polymer ratios were decided as the initial step of the QbD process. Three different polymer types (PLA, PEG, and PESu) and different polymer ratios (95, 90, and 50% for PLA and 5, 10, 50% for PEG or PESu) were considered as CMAs, and blends were prepared using this framework. Different effects of CMAs on predetermined CQAs were studied in the QbD framework.

In the Summary of Model output, Standard error of the regression (S), and determination coefficient (R-square) provide an overall measure of how well the model fits the data. S is known both as the standard error of the regression and as the standard error of the estimate. R-square is a proportion of the change in the output response which is predicted from the inputs (i.e., PLA, PEG, and PESu ratio). The adjusted R-square (R-square adj) is an updated version of the R-square that is adjusted for the number of factors in the model. The predictive R-square (R-square pred) demonstrates how well a regression predicts answers for new views[61]. In Table 7, it was demonstrated that all R-square values were higher than the %77. A higher value of R-square proves that more models have captured variation in the results; it demonstrates that the model is reliable[62].

When the coefficient term of the regression model is not different from 0 ($p > 0.05$), it shows that the response is not influenced by varying the input factor levels[61]. p-Values of the PLA factor are <0.05 for weight, thickness, tensile strength, Young's modulus, elongation, and drug content parameters. So, PLA is an efficient factor in these CQA parameters. p-Values of the PEG factor are higher than 0.05

Table 7. Model summary of topical PTX loaded films.

CQA	S	R-square (%)	R-square adj (%)	R-square pred (%)
Weight (mg)	1.35033	99.90	99.80	98.90
Thickness (mm)	0.016905	98.96	97.92	90.59
Water uptake (%)	0.904443	77.83	55.66	0.00
Hydrolysis (%)	6.51789	98.55	97.11	22.14
Moisture absorption (%)	0.315712	99.67	99.34	88.09
Moisture loss (%)	0.146159	99.73	99.46	99.46
Tensile strength (MPa)	1.8864	97.14	94.27	52.20
Young's modulus (MPa/%)	0.167648	99.06	98.11	75.91
Elongation at break (%)	6.11331	97.42	94.84	49.85
Drug content (%)	19.4098	96.68	93.36	38.12
Diss. 1 h	1.6265	99.46	98.92	97.66
Diss. 4 h	2.32061	99.66	99.32	95.62
Diss. 6 h	2.80585	99.56	99.12	88.06
Diss. 24 h	1.63996	99.91	99.82	99.73
Diss. 36 h	3.1735	99.76	99.53	97.69
Diss. 48 h	4.34669	99.63	99.27	84.25
Diss. 72 h	4.24443	99.68	99.36	83.13
Diss. 96 h	2.74995	99.88	99.76	94.89

Diss.: Dissolution.

Table 8. *p*-Values of PLA, PEG, and PESu on CQA parameters.

CQA	PLA	PEG	PESu
Weight	0.000	0.001	0.004
Thickness	0.002	0.128	0.009
Water uptake	0.081	0.067	0.498
Hydrolysis	0.521	0.001	0.012
Moisture absorption	0.054	0.000	0.003
Moisture loss	0.109	0.000	0.000
Tensile strength	0.002	0.350	0.088
Young modulus	0.001	0.629	0.053
Elongation at break	0.006	0.022	0.190
Drug content	0.037	0.024	0.029
Dis. 1 h	0.448	0.000	0.001
Dis. 4 h	0.098	0.000	0.000
Dis. 6 h	0.231	0.000	0.000
Dis. 24 h	0.139	0.000	0.000
Dis. 36 h	0.269	0.000	0.000
Dis. 48 h	0.712	0.000	0.000
Dis. 72 h	0.835	0.000	0.000
Dis. 96 h	0.704	0.000	0.000

($p > 0.05$) for thickness, water uptake, tensile strength, and Young's modulus. So, the PEG is an efficient factor in our CQA parameters except for these parameters. Table 8 demonstrates all *p*-values on CQA parameters.

p-Values of PESu are higher than 0.05 ($p > 0.05$) in many CQA parameters, such as water uptake, tensile strength, and elongation. It shows us these parameters are not affected by varying PESu levels. Consequently, it is crucial to control the polymer amount and polymer type because of different effects in the film, as the influences of CMA parameters can be seen through the concept of QbD. Contour plot graphics show the effect of various concentrations of PEG and PESu on weight, hydrolysis, moisture absorption, and moisture loss (Figure 6).

3.7. Determination of in vitro anticancer activity on MCF-7 and A549 cancer cell lines

According to the previous physicochemical examination and especially release profile, F9 and F12 formulations were selected to be studied for their *in vitro* anticancer activity against MCF-7 and A549 cell lines. Figure 7 depicts the morphology of the F9 and F12 films studied by SEM and Fluorescence Microscopy methods. In the case of F12, phase separation has occurred since the PESu phase is dispersed into the PLA matrix[17] while for the F9 films a porous structure is obtained. The phase separation can be identified by the empty spaces of PEG scattered throughout the PLA matrix. In general, immiscible polymer blends lead to porosity, and empty spaces between the polymer phases as previous studies have stated[17]. A recent study showed that PDLA and PEG (15,000) films present porous structures with the diameter of the holes in these samples reaching 0.5–1 µm. In addition, the holes were evenly distributed across the surface of the film. Both PLA and PEG affect the morphology of the surface films[63].

According to our previous study, PLA/PESu blends are biocompatible; thus their possible application would not lead to any undesirable toxic effects[17]. Moreover, PLA/PEG blends have been studied by different research groups revealing their biocompatibility[64]. Therefore, in this work, the developed films were studied for their *in vitro* anticancer activity.

Taxol® is widely used as a first-line chemotherapy agent in the treatment of multiple types of tumors, including non-small cell lung cancer[65] and breast cancer[66]. *In vitro* anticancer activity of newly developed formulations can be performed using various tests. Endpoint analysis (MTT, XTT, etc.) are relatively cheaper, simpler, and faster method compared to other methods in terms of analyzing the effects of many compounds in very different concentrations. Despite these advantages, there are many experimental problems in endpoint methods. The biggest challenge relates to time optimization. Many cell lines may begin to proliferate later than the time interval selected for spectrophotometric reading. Also, low concentrations of toxic substances can stimulate cell activation. Different results can be obtained at different incubation times, which creates problems for reliability. The results obtained in tetrazolium salts methods (MTT etc.) show cytotoxicity only at a one-time point and there is no possibility to see any cellular changes between time points during an experiment. A major disadvantage of tetrazolium salt methods is that the formazan products react with the substances present or tested in the culture medium

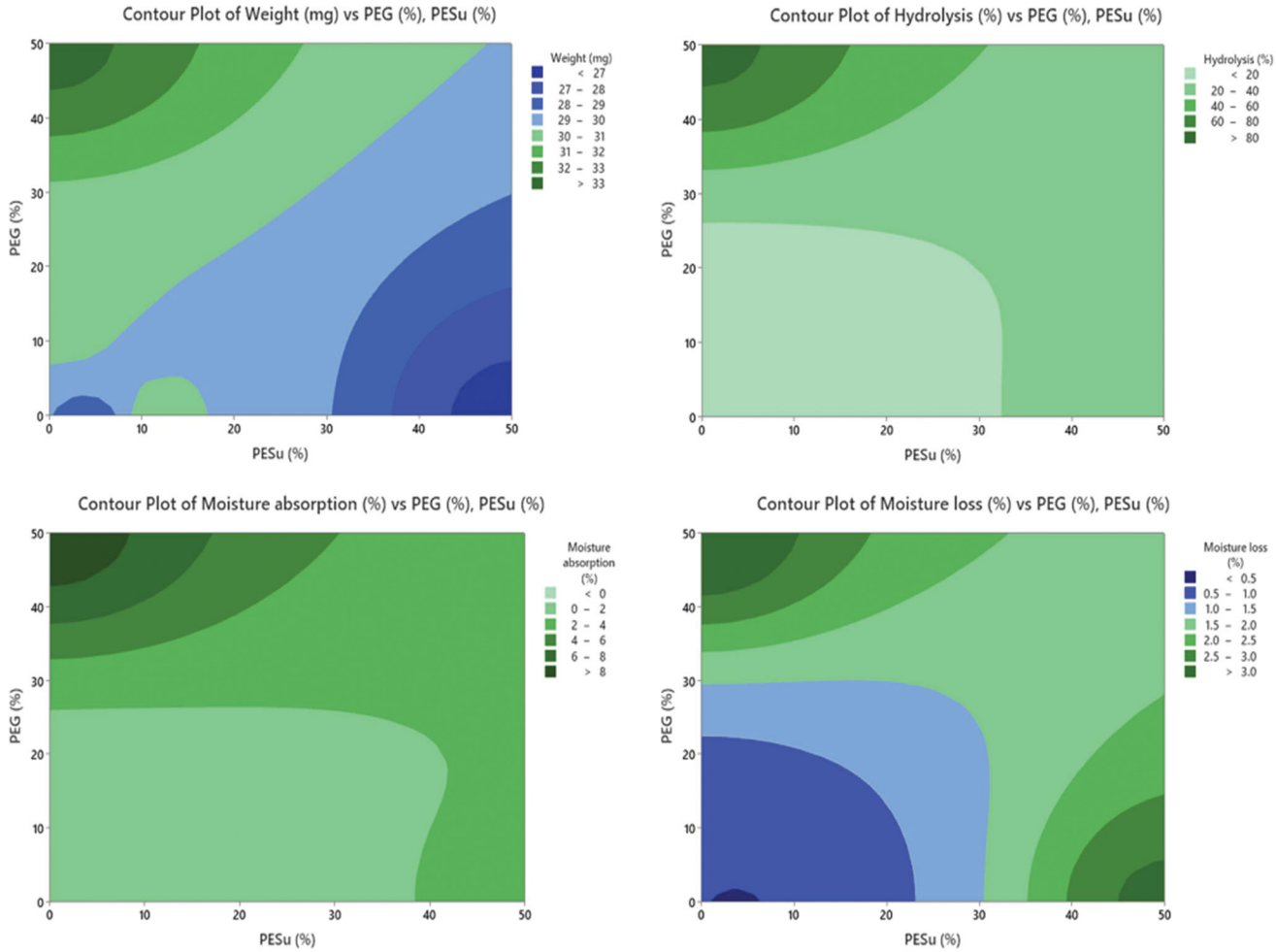

Figure 6. Contour plot graphics of various concentrations of PEG and PESu on weight, hydrolysis, moisture uptake and moisture loss *vs.* weight, hydrolysis, moisture absorption, and moisture loss drug loading of topical PTX loaded films.

during the experiment. Therefore, the test can give false-positive results. Impedance-based technology (xCELLigence) allows us to measure an entire experiment at multiple time points and creates curves that reflect cellular proliferation, growth, and morphological changes before and after adding a compound. The data obtained allow the calculation of the IC50 and EC50 at each time point of the experiment. The system is very useful in screening new potential cytotoxic drugs because it shows the effect of a compound on cells in real-time. In impedance-based measurement systems, since there is no substance to react with the substance to be tested, there is no possibility of such a wrong result in these systems[67]. As a result, although a real-time cell analysis system (xCELLigence) is an expensive method, it is a modern and useful technique due to continuous and real-time monitoring of cell proliferation and cellular morphological changes. Based on the explained characteristics of these analyses, xCELLigence was chosen for the cell viability test.

Herein, the cytotoxicity of F9, F12 formulations, and PTX was evaluated in human lung and breast cancer cell lines (A549 and MCF 7) within the range of 0–1,000 nM. Based on the results of our previous characterization test, F9 and F12 (which have maximum and faster PTX release) formulations were chosen for cytotoxicity assay. After the cells were treated with F9, F12, and PTX (100, 500, and 1,000 nM) the viabilities in cells were detected and demonstrated in Figures 8 and 9. According to the results, for the tested concentrations until 72 h, the cell viability of F9, F12, and PTX was generally higher on A549 cell lines when compared to MCF-7 cell lines. The cell viability usually displayed a decrease by the increase in the concentrations, as expected. Both formulations acted better against the MCF7 cell lines than A549 cells. Moreover, PTX formulations retain cytotoxic activity since they inhibit the growth of cancer cells even after 96 h. In the past, polymeric expansile nanoparticles loaded with PTX showed anticancer efficacy against various breast cancer cells including MCF7[68]. Similarly, PTX-loaded keratin nanoparticles were studied in two-dimensional (MCF-7 and MDA MB 231 cell lines) and perfused three-dimensional breast cancer models. It was revealed that the formulations were able to inhibit tumor cell viability and induce apoptosis[69]. In the case of A549 cells, F9 and F12 showed similar inhibitory effects with PTX. However, even PTX was not as effective as it was expected. It has been reported that A549 cells can resist PTX activity to retain their viability[70]. Normally such

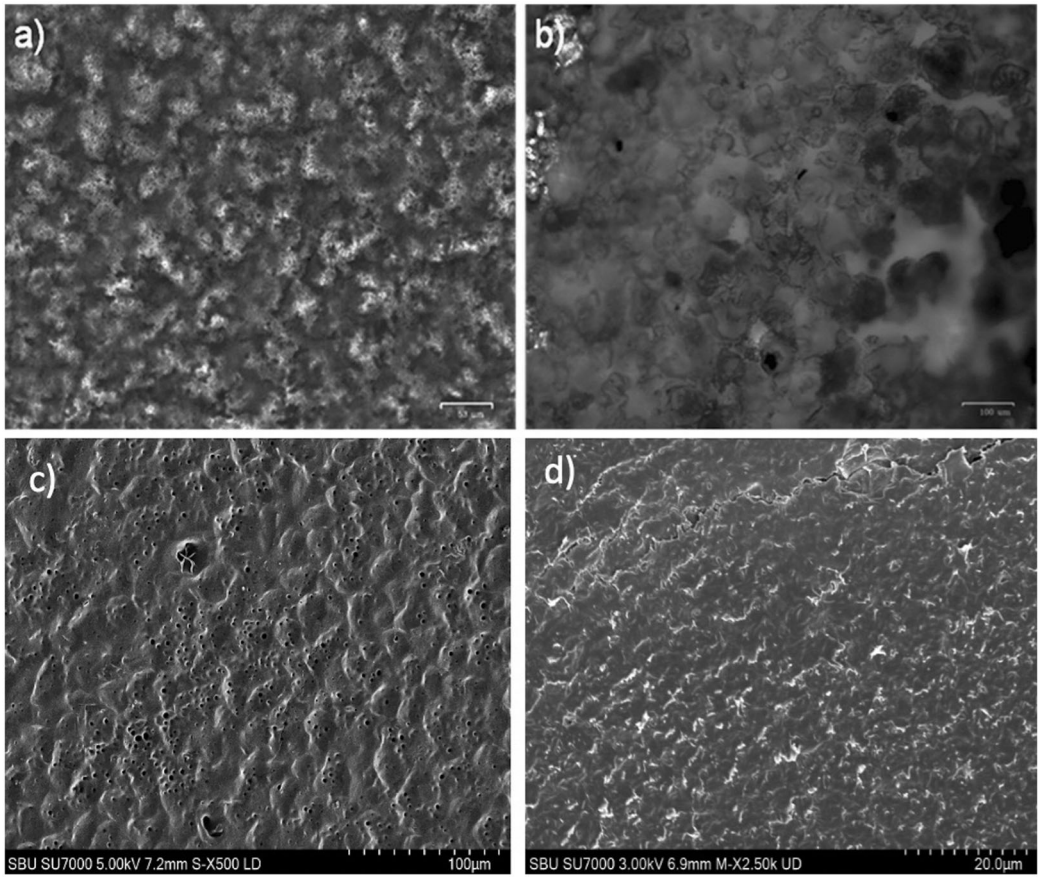

Figure 7. Morphology of (a) F9 and (b) F12 films derived from ZOE Fluorescent Cell Imager microscope, (c) F9 and (d) F12 derived from Scanning Electron Microscopy.

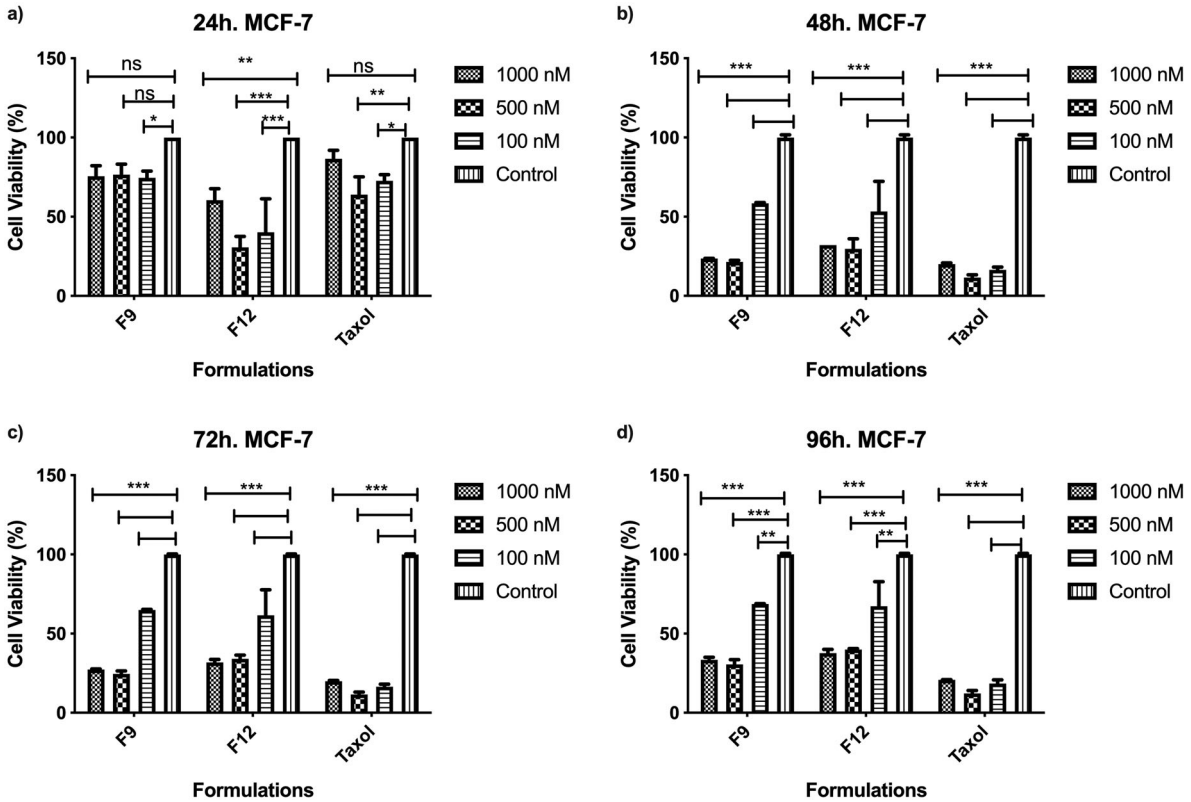

Figure 8. *In vitro* cell viability studies after treatment of MCF-7 cells with F9 and F12 at (a) 24 h, (b) 48 h, (c) 72 h, and (d) 96 h (***$p < 0.001$, **$p < 0.01$, *$p < 0.05$, $^{ns}p > 0.05$, relative to control).

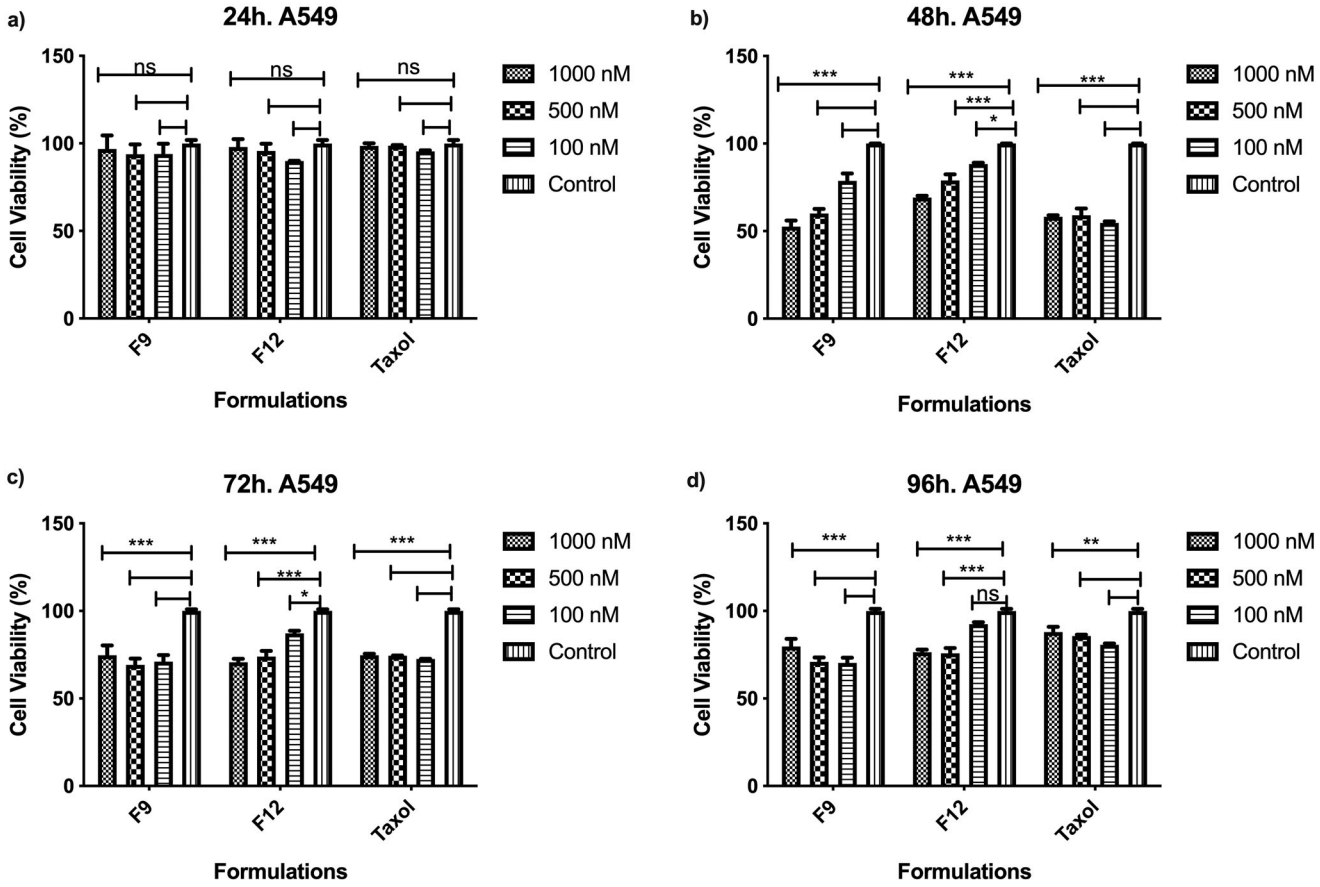

Figure 9. *In vitro* cell viability studies after treatment of A549 cells with F9 and F12 at (a) 24 h, (b) 48 h, (c) 72 h, and (d) 96 h (***$p < 0.001$, **$p < 0.01$, *$p < 0.05$, $^{ns}p > 0.05$, relative to control).

resistance can be overcome using various methodologies which will be the subject of future studies.

4. Conclusion

Herein, the preparation and characterization of PLA and its blends with PESu and PEG are discussed as potential implants against breast and lung cancer. The matrices as topical implants were developed via the easy and cost-effective solvent evaporation method. The well-known antitumor drug, PTX was used as a model drug. According to the physicochemical characterization immiscible and partially miscible blends were developed as FTIR and DSC studies indicated. Water uptake and degree of hydrolysis showed that the addition of PEG led to improved solubility of the film while PESu enhanced the degradation rate. As the PEG and PESu ratio in the films increased, the release rate increased. PTX was incorporated into the blends in the amorphous state which led to improved dissolution; the amorphization of the drug was not correlated with chemical interactions between polymer and drugs. Nonetheless, the blends present different release patterns and hydrolysis rates analogous to the concentrations of the polymers. At the end of the research, it was seen that the QbD approach can be useful in improving the process and product understanding. The application of QbD will enable an understanding of the importance of some material parameters in the formulation process. It has been observed that the change in the type and ratio of the polymers used with the QbD approach affects the critical properties. *In vitro* cell viability studies depicted that F9 (PLA/PEG-50/50) and F12 (PLA/PESu-50/50) showed improved anticancer activity on MCF-7 cell lines but poor anticancer activity on A549 cells. As expected, cell viability decreased by increasing the concentration of the formulation. The prepared films can be alternatively used as promising topical implants for improved anticancer activity against breast and lung cancer.

Disclosure statement

The authors declare no conflict of interest.

Funding

This research did not receive any specific grant from funding agencies in the public, commercial, or not-for-profit sectors.

ORCID

Ece Özcan Bülbül http://orcid.org/0000-0001-7112-923X
Neslihan Üstündağ Okur http://orcid.org/0000-0002-3210-3747
Panoraia I. Siafaka http://orcid.org/0000-0001-7256-3230

References

[1] World Health Organization. Cancer. https://www.who.int/news-room/fact-sheets/detail/cancer (accessed Jul 20, 2020).

[2] Başpı nar, Y.; Erel-Akbaba, G.; Kotmakçı , M.; Akbaba, H. Development and Characterization of Nanobubbles Containing Paclitaxel and Survivin Inhibitor YM155 against Lung Cancer. *Int. J. Pharm.* **2019**, *566*, 149–156. DOI: 10.1016/j.ijpharm.2019.05.039.

[3] Lin, H.; Hu, B.; He, X.; Mao, J.; Wang, Y.; Wang, J.; Zhang, T.; Zheng, J.; Peng, Y.; Zhang, F. Overcoming Taxol-Resistance in A549 Cells: A Comprehensive Strategy of Targeting P-Gp Transporter, AKT/ERK Pathways, and Cytochrome P450 Enzyme CYP1B1 by 4-Hydroxyemodin. *Biochem. Pharmacol.* **2020**, *171*, 113733. DOI: 10.1016/j.bcp.2019.113733.

[4] Harbeck, N.; Penault-Llorca, F.; Cortes, J.; Gnant, M.; Houssami, N.; Poortmans, P.; Ruddy, K.; Tsang, J.; Cardoso, F. Breast Cancer. *Nat. Rev. Dis. Primers* **2019**, *5*, 66. DOI: 10.1038/s41572-019-0111-2.

[5] Comşa, Ş.; Cîmpean, A. M.; Raica, M. The Story of MCF-7 Breast Cancer Cell Line: 40 Years of Experience in Research. *Anticancer Res.* **2015**, *35*, 3147–3154.

[6] Osborne, C. K.; Hobbs, K.; Trent, J. M. Biological Differences among MCF-7 Human Breast Cancer Cell Lines from Different Laboratories. *Breast Cancer Res. Treat.* **1987**, *9*, 111–121. DOI: 10.1007/BF01807363.

[7] Amin, R.; Morita-fujimura, Y.; Tawarayama, H.; Semba, K.; Chiba, N.; Fukumoto, M.; Ikawa, S. Np63 a Induces Quiescence and Downregulates the BRCA1 Pathway in Estrogen Receptor-Positive Luminal Breast Cancer Cell Line MCF7 but Not in Other Breast Cancer Cell Lines. *Mol. Oncol.* **2016**, *10*, 575–593. DOI: 10.1016/j.molonc.2015.11.009.

[8] Costa, B.; Amorim, I.; Gärtner, F.; Vale, N. Understanding Breast Cancer: From Conventional Therapies to Repurposed Drugs. *Eur. J. Pharm. Sci.* **2020**, *151*, 105401. DOI: 10.1016/j.ejps.2020.105401.

[9] Dhanikula, A. B.; Panchagnula, R. Development and Characterization of Biodegradable Chitosan Films for Local Delivery of Paclitaxel. *AAPS J.* **2004**, *6*, 88–99. DOI: 10.1208/aapsj060327.

[10] Rong, H.-J.; Chen, W.-L.; Guo, S.-R.; Lei, L.; Shen, Y.-Y. PCL Films Incorporated with Paclitaxel/5-Fluorouracil: Effects of Formulation and Spacial Architecture on Drug Release. *Int. J. Pharm.* **2012**, *427*, 242–251. DOI: 10.1016/j.ijpharm.2012.02.007.

[11] Krukiewicz, K.; Zak, J. K. Biomaterial-Based Regional Chemotherapy: Local Anticancer Drug Delivery to Enhance Chemotherapy and Minimize Its Side-Effects. *Mater. Sci. Eng. C Mater. Biol. Appl.* **2016**, *62*, 927–942. DOI: 10.1016/j.msec.2016.01.063.

[12] Özcan Bülbül, E.; Mesut, B.; Cevher, E.; Öztaş, E.; Özsoy, Y. Product Transfer from Lab-Scale to Pilot-Scale of Quetiapine Fumarate Orodispersible Films Using Quality by Design Approach. *J. Drug Deliv. Sci. Technol.* **2019**, *54*, 101358. DOI: 10.1016/j.jddst.2019.101358.

[13] Jani, R.; Patel, D. Hot Melt Extrusion: An Industrially Feasible Approach for Casting Orodispersible Film. *Asian J. Pharm. Sci.* **2015**, *10*, 292–305. DOI: 10.1016/j.ajps.2015.03.002.

[14] ICH Q8(R2). *ICH Harmonised Tripartite Guideline Pharmaceutical Development Q8(R2)*; 2009.

[15] Mazumder, S.; Pavurala, N.; Manda, P.; Xu, X.; Cruz, C. N.; Krishnaiah, Y. S. R. Quality by Design Approach for Studying the Impact of Formulation and Process Variables on Product Quality of Oral Disintegrating Films. *Int. J. Pharm.* **2017**, *527*, 151–160. DOI: 10.1016/j.ijpharm.2017.05.048.

[16] Krull, S. M.; Patel, H. V.; Li, M.; Bilgili, E.; Dave, R. N. Critical Material Attributes (CMAs) of Strip Films Loaded with Poorly Water-Soluble Drug Nanoparticles: I. Impact of Plasticizer on Film Properties and Dissolution. *Eur. J. Pharm. Sci.* **2016**, *92*, 146–155. DOI: 10.1016/j.ejps.2016.07.005.

[17] Üstündağ Okur, N.; Filippousi, M.; Okur, M. E.; Ayla, Ş.; Çağlar, E. Ş.; Yoltaş, A.; Siafaka, P. I. A Novel Approach for Skin Infections: Controlled Release Topical Mats of Poly(Lactic Acid)/Poly(Ethylene Succinate) Blends Containing Voriconazole. *J. Drug Deliv. Sci. Technol.* **2018**, *46*, 74–86. DOI: 10.1016/j.jddst.2018.05.005.

[18] Siafaka, P. I. P. I.; Barmbalexis, P.; Bikiaris, D. N. D. N. Novel Electrospun Nanofibrous Matrices Prepared from Poly(Lactic Acid)/Poly(Butylene Adipate) Blends for Controlled Release Formulations of an Anti-Rheumatoid Agent. *Eur. J. Pharm. Sci.* **2016**, *88*, 12–25. DOI: 10.1016/j.ejps.2016.03.021.

[19] Üstündağ Okur, N.; Hökenek, N.; Okur, M. E.; Ayla, Ş.; Yoltaş, A.; Siafaka, P. I.; Cevher, E. An Alternative Approach to Wound Healing Field; New Composite Films from Natural Polymers for Mupirocin Dermal Delivery. *Saudi Pharm. J.* **2019**, *27*, 738–752. DOI: 10.1016/j.jsps.2019.04.010.

[20] Pekoz, A. Y.; Erdal, M. S.; Okyar, A.; Ocak, M.; Tekeli, F.; Kaptan, E.; Sagirli, O.; Araman, A. Preparation and *In-Vivo* Evaluation of Dimenhydrinate Buccal Mucoadhesive Films with Enhanced Bioavailability. *Drug Dev. Ind. Pharm.* **2016**, *42*, 916–925. DOI: 10.3109/03639045.2015.1091470.

[21] Kim, S. Y.; Hwang, J. Y.; Seo, J. W.; Shin, U. S. Production of CNT-Taxol-Embedded PCL Microspheres Using an Ammonium-Based Room Temperature Ionic Liquid: As a Sustained Drug Delivery System. *J. Colloid Interface Sci.* **2015**, *442*, 147–153. DOI: 10.1016/j.jcis.2014.11.044.

[22] Feng, S. s.; Huang, G. Effects of Emulsifiers on the Controlled Release of Paclitaxel (Taxol®) from Nanospheres of Biodegradable Polymers. *J. Control. Release* **2001**, *71*, 53–69. DOI: 10.1016/S0168-3659(00)00364-3.

[23] Mu, L.; Feng, S. S. A Novel Controlled Release Formulation for the Anticancer Drug Paclitaxel (Taxol®): PLGA Nanoparticles Containing Vitamin E TPGS. *J. Control. Release* **2003**, *86*, 33–48. DOI: 10.1016/S0168-3659(02)00320-6.

[24] Hobzova, R.; Hampejsova, Z.; Cerna, T.; Hrabeta, J.; Venclikova, K.; Jedelska, J.; Bakowsky, U.; Bosakova, Z.; Lhotka, M.; Vaculin, S.; et al. Poly(D,L-Lactide)/Polyethylene Glycol Micro/Nanofiber Mats as Paclitaxel-Eluting Carriers: Preparation and Characterization of Fibers, *In Vitro* Drug Release, Antiangiogenic Activity and Tumor Recurrence Prevention. *Mater. Sci. Eng. C Mater. Biol. Appl.* **2019**, *98*, 982–993. DOI: 10.1016/j.msec.2019.01.046.

[25] Filippousi, M.; Papadimitriou, S. A.; Bikiaris, D. N.; Pavlidou, E.; Angelakeris, M.; Zamboulis, D.; Tian, H.; Van Tendeloo, G. Novel Core-Shell Magnetic Nanoparticles for Taxol Encapsulation in Biodegradable and Biocompatible Block Copolymers: Preparation, Characterization and Release Properties. *Int. J. Pharm.* **2013**, *448*, 221–230. DOI: 10.1016/j.ijpharm.2013.03.025.

[26] Dash, S.; Murthy, P. N.; Nath, L.; Chowdhury, P. Kinetic Modeling on Drug Release from Controlled Drug Delivery Systems. *Acta Pol. Pharm. Drug Res.* **2010**, *67*, 217–223.

[27] Aksu, B.; Yurdasiper, A.; Ege, M. A.; Okur, N. Ü.; Yesim, H. Development and Comparative Evaluation of Extended Release Indomethacin Capsules. *African J. Pharm. Pharmacol.* **2013**, *7*, 2201–2209.

[28] Costa, P.; Lobo, J. M. S. Modeling and Comparison of Dissolution Profiles. *Eur. J. Pharm. Sci.* **2001**, *13*, 123–133. DOI: 10.1016/S0928-0987(01)00095-1.

[29] Siafaka, P. I.; Barmpalexis, P.; Lazaridou, M.; Papageorgiou, G. Z.; Koutris, E.; Karavas, E.; Kostoglou, M.; Bikiaris, D. N. Controlled Release Formulations of Risperidone Antipsychotic Drug in Novel Aliphatic Polyester Carriers: Data Analysis and Modelling. *Eur. J. Pharm. Biopharm.* **2015**, *94*, 473–484. DOI: 10.1016/j.ejpb.2015.06.027.

[30] Karavas, E.; Georgarakis, E.; Bikiaris, D. Adjusting Drug Release by Using Miscible Polymer Blends as Effective Drug Carries. *J. Therm. Anal. Calorim.* **2006**, *84*, 125–133. DOI: 10.1007/s10973-005-7193-7.

[31] Lyu, S. P.; Sparer, R.; Hobot, C.; Dang, K. Adjusting Drug Diffusivity Using Miscible Polymer Blends. *J. Control. Release* **2005**, *102*, 679–687. DOI: 10.1016/j.jconrel.2004.11.007.

[32] Kolbuk, D.; Sajkiewicz, P.; Denis, P.; Choinska, E. Investigations of Polycaprolactone/Gelatin Blends in Terms of Their Miscibility. *Bull. Polish Acad. Sci. Tech. Sci.* **2013**, *61*, 629–632.

[33] Wagner, A.; Poursorkhabi, V.; Mohanty, A. K.; Misra, M. Analysis of Porous Electrospun Fibers from Poly(L-Lactic Acid)/Poly(3-Hydroxybutyrate-Co-3-Hydroxyvalerate) Blends. *ACS Sustain. Chem. Eng.* **2014**, *2*, 1976–1982. DOI: 10.1021/sc5000495.

[34] Pivsa-Art, W.; Fujii, K.; Nomura, K.; Aso, Y.; Ohara, H.; Yamane, H. The Effect of Poly(Ethylene Glycol) as Plasticizer in Blends of Poly(Lactic Acid) and Poly(Butylene Succinate). *J. Appl. Polym. Sci.* **2016**, *43044*, 1–10.

[35] Qiu, Z.; Komura, M.; Ikehara, T.; Nishi, T. DSC and TMDSC Study of Melting Behaviour of Poly(Butylene Succinate) and Poly(Ethylene Succinate). *Polymer* **2003**, *44*, 7781–7785. DOI: 10.1016/j.polymer.2003.10.045.

[36] Chieng, B. W.; Ibrahim, N. A.; Yunus, W. M. Z. W.; Hussein, M. Z. Poly(Lactic Acid)/Poly(Ethylene Glycol) Polymer Nanocomposites: Effects of Graphene Nanoplatelets. *Polymers* **2013**, *6*, 93–104. DOI: 10.3390/polym6010093.

[37] Siafaka, P. I.; Betsiou, M.; Tsolou, A.; Angelou, E.; Agianian, B.; Koffa, M.; Chaitidou, S.; Karavas, E.; Avgoustakis, K.; Bikiaris, D. Synthesis of Folate- Pegylated Polyester Nanoparticles Encapsulating Ixabepilone for Targeting Folate Receptor Overexpressing Breast Cancer Cells. *J. Mater. Sci. Mater. Med.* **2015**, *26*, 1–14.

[38] Woo, E. M.; Hsieh, Y.-T.; Chen, W.-T.; Kuo, N.-T.; Wang, L.-Y. Immiscibility-Miscibility Phase Transformation in Blends of Poly(Ethylene Succinate) with Poly(L-Lactic Acid)s of Different Molecular Weights. *J. Polym. Sci. B Polym. Phys.* **2010**, *48*, 1135–1147. DOI: 10.1002/polb.21999.

[39] Hiremath, J. G.; Khamar, N. S.; Palavalli, S. G.; Rudani, C. G.; Aitha, R.; Mura, P. Paclitaxel Loaded Carrier Based Biodegradable Polymeric Implants: Preparation and *In Vitro* Characterization. *Saudi Pharm. J.* **2013**, *21*, 85–91. DOI: 10.1016/j.jsps.2011.12.002.

[40] Yang, F. H.; Zhang, Q.; Liang, Q. Y.; Wang, S. Q.; Zhao, B. X.; Wang, Y. T.; Cai, Y.; Li, G. F. Bioavailability Enhancement of Paclitaxel via a Novel Oral Drug Delivery System: Paclitaxel-Loaded Glycyrrhizic Acid Micelles. *Molecules* **2015**, *20*, 4337–4356. DOI: 10.3390/molecules20034337.

[41] Nanaki, S.; Siafaka, P. I.; Zachariadou, D.; Nerantzaki, M.; Giliopoulos, D. J.; Triantafyllidis, K. S.; Kostoglou, M.; Nikolakaki, E.; Bikiaris, D. N. PLGA/SBA-15 Mesoporous Silica Composite Microparticles Loaded with Paclitaxel for Local Chemotherapy. *Eur. J. Pharm. Sci.* **2017**, *99*, 32–44. DOI: 10.1016/j.ejps.2016.12.010.

[42] Karki, S.; Kim, H.; Na, S.-J.; Shin, D.; Jo, K.; Lee, J. Thin Films as an Emerging Platform for Drug Delivery. *Asian J. Pharm. Sci.* **2016**, *11*, 559–574. DOI: 10.1016/j.ajps.2016.05.004.

[43] Nair, A. B.; Kumria, R.; Harsha, S.; Attimarad, M.; Al-Dhubiab, B. E.; Alhaider, I. A. *In Vitro* Techniques to Evaluate Buccal Films. *J. Control. Release* **2013**, *166*, 10–21. DOI: 10.1016/j.jconrel.2012.11.019.

[44] Tong, Q.; Xiao, Q.; Lim, L. T. Preparation and Properties of Pullulan-Alginate-Carboxymethylcellulose Blend Films. *Food Res. Int.* **2008**, *41*, 1007–1014. DOI: 10.1016/j.foodres.2008.08.005.

[45] Namdeo, A.; Garud, N.; Garud, A. Development and Evaluation of Transdermal Patches of Quetiapine Fumerate for the Treatment of Psychosis. *Int. J. Drug Deliv.* **2012**, *4*, 470–476.

[46] Cilurzo, F.; Cupone, I. E.; Minghetti, P.; Buratti, S.; Gennari, C. G. M.; Montanari, L. Diclofenac Fast-Dissolving Film: Suppression of Bitterness by a Taste-Sensing System. *Drug Dev. Ind. Pharm.* **2011**, *37*, 252–259. DOI: 10.3109/03639045.2010.505928.

[47] Gal, A.; Nussinovitch, A. Plasticizers in the Manufacture of Novel Skin-Bioadhesive Patches. *Int. J. Pharm.* **2009**, *370*, 103–109. DOI: 10.1016/j.ijpharm.2008.11.015.

[48] Rahman, M.; Brazel, C. S. The Plasticizer Market: An Assessment of Traditional Plasticizers and Research Trends to Meet New Challenges. *Prog. Polym. Sci.* **2004**, *29*, 1223–1248. DOI: 10.1016/j.progpolymsci.2004.10.001.

[49] Güngör, S.; Erdal, M. S.; Özsoy, Y. Plastizers in Transdermal Drug Delivery Systems. In *Recent Advances in Plastizers*; Luqman, M., Ed.; In Tech: Croatia, 2012; pp 91–112.

[50] Lu, J.; Qiu, Z.; Yang, W. Fully Biodegradable Blends of Poly (L-Lactide) and Poly (Ethylene Succinate): Miscibility, Crystallization, and Mechanical Properties. *Polymer* **2007**, *48*, 4196–4204. DOI: 10.1016/j.polymer.2007.05.035.

[51] Miao, L.; Qiu, Z.; Yang, W.; Ikehara, T. Fully Biodegradable Poly (3-Hydroxybutyrate-Co-Hydroxyvalerate)/Poly (Ethylene Succinate) Blends: Phase Behavior, Crystallization and Mechanical Properties. *React. Funct. Polym.* **2008**, *68*, 446–457. DOI: 10.1016/j.reactfunctpolym.2007.11.001.

[52] Cai, Q.; Bei, J.; Wang, S. *In Vitro* Study on the Drug Release Behavior from Polylactide-Based Blend Matrices. *Polym. Adv. Technol.* **2002**, *13*, 534–540. DOI: 10.1002/pat.222.

[53] Fu, Y.; Kao, W. J. Drug Release Kinetics and Transport Mechanisms of Non-Degradable and Degradable Polymeric Delivery Systems. *Expert Opin. Drug Deliv.* **2010**, *7*, 429–444. DOI: 10.1517/17425241003602259.

[54] Mathematical Models of drug release. In *Strategies to Modify the Drug Release from Pharmaceutical Systems*; Bruschi, M. L., Ed.; Woodhead Publishing: Cambridge, 2015; pp 63–86.

[55] Alaee, M.; Moghadam, S. H.; Sayyar, P.; Atyabi, F.; Dinarvand, R. Preparation of a Reservoir Type Levonorgestrel Delivery System Using High Molecular Weight Poly L-Lactide. *Iran. J. Pharm. Res.* **2009**, *8*, 87–93.

[56] Mostafavi, S.; Karkhane, R.; Riazi-Esfahani, M.; Dorkoosh, F.; Rafiee-Tehrani, M.; Tamaddon, L. Design and Development of Intraocular Polymeric Implant Systems for Long-Term Controlled-Release of Clindamycin Phosphate for Toxoplasmic Retinochoroiditis. *Adv. Biomed. Res.* **2015**, *4*, 32. DOI: 10.4103/2277-9175.150426.

[57] Wojcik-Pastuszka, D.; Krzak, J.; Macikowski, B.; Berkowski, R.; Osiński, B.; Musiał, W. Evaluation of the Release Kinetics of a Pharmacologically Active Substance from Model Intra-Articular Implants Replacing the Cruciate Ligaments of the Knee. *Materials* **2019**, *12*, 1202. DOI: 10.3390/ma12081202.

[58] Siafaka, P.; Okur, M. E.; Ayla, Ş.; Er, S.; Cağlar, E. Ş.; Okur, N. Ü. Design and Characterization of Nanocarriers Loaded with Levofloxacin for Enhanced Antimicrobial Activity; Physicochemical Properties, *In Vitro* Release and Oral Acute Toxicity. *Braz. J. Pharm. Sci.* **2019**, *55*, 1–13.

[59] Üstündağ-Okur, N.; Gökçe, E. H.; Bozbıyık, D. İ.; Eğrilmez, S.; Ertan, G.; Özer, Ö. Novel Nanostructured Lipid Carrier-Based Inserts for Controlled Ocular Drug Delivery: Evaluation of Corneal Bioavailability and Treatment Efficacy in Bacterial Keratitis. *Expert Opin. Drug Deliv.* **2015**, *12*, 1791–1807. DOI: 10.1517/17425247.2015.1059419.

[60] Ramyadevi, D.; Rajan, K. S. Interaction and Release Kinetics Study of Hybrid Polymer Blend Nanoparticles for PH Independent Controlled Release of an Anti-Viral Drug. *J. Taiwan Inst. Chem. Eng.* **2015**, *50*, 1–11. DOI: 10.1016/j.jtice.2014.12.036.

[61] Fukuda, I. M.; Pinto, C. F. F.; Moreira, C. D. S.; Saviano, A. M.; Lourenço, F. R. Design of Experiments (DoE) Applied to Pharmaceutical and Analytical Quality by Design (QbD). *Braz. J. Pharm. Sci.* **2018**, *54*, 1–16.

[62] Amasya, G.; Badilli, U.; Aksu, B.; Tarimci, N. Quality by Design Case Study 1: Design of 5-Fl Uorouracil Loaded Lipid Nanoparticles by the W/O/W Double Emulsion — Solvent Evaporation Method. *Eur. J. Pharm. Sci.* **2016**, *84*, 92–102. DOI: 10.1016/j.ejps.2016.01.003.

[63] Nashchekina, Y.; Nikonov, P.; Nashchekin, A.; Mikhailova, N. Functional Polylactide Blend Films for Controlling Mesenchymal Stem Cell Behaviour. *Polymers* **2020**, *12*, 1969. DOI: 10.3390/polym12091969.

[64] Vasile, C.; Stoleru, E.; Darie-Niţa, R. N.; Dumitriu, R. P.; Pamfil, D.; Tarţau, L. Biocompatible Materials Based on Plasticized Poly(Lactic Acid), Chitosan and Rosemary Ethanolic Extract I. Effect of Chitosan on the Properties of Plasticized Poly(Lactic Acid) Materials. *Polymers* **2019**, *11*, 941. DOI: 10.3390/polym11060941.

[65] Li, X.; Yang, B.; Ren, H.; Xiao, T.; Zhang, L.; Li, L.; Li, M.; Wang, X.; Zhou, H.; Zhang, W. Hsa_Circ_0002483 Inhibited the Progression and Enhanced the Taxol Sensitivity of Non-Small Cell Lung Cancer by Targeting MiR-182-5p. *Cell Death Dis.* **2019**, *10*, 953. DOI: 10.1038/s41419-019-2180-2.

[66] Sparano, J. A.; Wang, M.; Martino, S.; Jones, V.; Perez, E. A.; Saphner, T.; Wolff, A. C.; Sledge, G. W.; Wood, W. C.; Davidson, N. E. Weekly Paclitaxel in the Adjuvant Treatment of Breast Cancer. *N. Engl. J. Med.* **2008**, *358*, 1663–1671. DOI: 10.1056/NEJMoa0707056.

[67] Stefanowicz-hajduk, J.; Ochocka, J. R. Real-Time Cell Analysis System in Cytotoxicity Applications: Usefulness and Comparison with Tetrazolium Salt Assays. *Toxicol. Rep.* **2020**, *7*, 335–344. DOI: 10.1016/j.toxrep.2020.02.002.

[68] Zubris, K. A. V.; Liu, R.; Colby, A.; Schulz, M. D.; Colson, Y. L.; Grinstaff, M. W. *In Vitro* Activity of Paclitaxel-Loaded Polymeric Expansile Nanoparticles in Breast Cancer Cells. *Biomacromolecules* **2013**, *14*, 2074–2082. DOI: 10.1021/bm400434h.

[69] Foglietta, F.; Spagnoli, G. C.; Muraro, M. G.; Ballestri, M.; Guerrini, A.; Ferroni, C.; Aluigi, A.; Sotgiu, G.; Varchi, G. Anticancer Activity of Paclitaxel-Loaded Keratin Nanoparticles in Two-Dimensional and Perfused Three-Dimensional Breast Cancer Models. *Int. J. Nanomedicine* **2018**, *13*, 4847–4867. volumeDOI: 10.2147/IJN.S159942.

[70] Xu, R.; Mao, Y.; Chen, K.; He, W.; Shi, W.; Han, Y. The Long Noncoding RNA ANRIL Acts as an Oncogene and Contributes to Paclitaxel Resistance of Lung Adenocarcinoma A549 Cells. *Oncotarget* **2017**, *8*, 39177–39184. DOI: 10.18632/oncotarget.16640.